Quasielastic Neutron Scattering in the High-Field Phase of a Haldane Antiferromagnet

A. Zheludev,[1,*] Z. Honda,[2] Y. Chen,[3] C. L. Broholm,[3,4] K. Katsumata,[5] and S. M. Shapiro[1]

[1]*Physics Department, Brookhaven National Laboratory, Upton, New York 11973-5000*
[2]*Faculty of Engineering, Saitama University, Urawa, Saitama 338-8570, Japan*
[3]*Department of Physics and Astronomy, Johns Hopkins University, Baltimore, Maryland 21218*
[4]*NIST Center for Neutron Research, National Institute of Standards and Technology, Gaithersburg, Maryland 20899*
[5]*The RIKEN Harima Institute, Mikazuki, Sayo, Hyogo 679-5148, Japan*

(Received 19 July 2001; published 5 February 2002)

Inelastic neutron scattering experiments on the Haldane-gap quantum antiferromagnet $Ni(C_5D_{14}N_2)_2N_3(PF_6)$ are performed in magnetic fields below and above the critical field H_c at which the gap closes. Quasielastic neutron scattering is found for $H > H_c$, indicating topological excitations in the high-field phase.

DOI: 10.1103/PhysRevLett.88.077206 PACS numbers: 75.50.Ee, 75.10.Jm, 75.40.Gb

As first realized by Haldane, integer-spin one-dimensional (1D) Heisenberg antiferromagnets (AFs) are exotic "quantum spin liquids" with only short-range spin correlations and a gap in the magnetic excitation spectrum [1]. Haldane-gap systems exhibit numerous unusual properties, and particularly interesting predictions were made for their behavior in high magnetic fields [2–7]. In an external field the gap excitations, which are a $S = 1$ triplet, are subject to Zeeman splitting. The gap Δ for one of the three branches decreases with field [Fig. 1(a)] and closes at some critical field $H_c \sim \Delta/g\mu_B$ [2–4,8]. Near H_c, this problem is equivalent to Bose condensation [3,4]. However, at $H > H_c$ the formation of a condensate is prevented by strong interactions between magnons. As a result, the high-field phase is rather unusual, with power-law spin correlations, and is an example of a *Luttinger spin liquid* [6,7]. The basic physics at $H > H_c$ can be understood within a simple model. The magnon interactions are assumed to be a hard-core repulsion, in which case the excitations behave as free fermions [3,4,9,10]. At $H > H_c$, the ground state is a Fermi sea of excitations with field-dependent Fermi density and wave vector q_F, as illustrated in Fig. 1(b). The spectrum is gapless, and dynamic spin correlations are incommensurate. The effect is related to field-induced incommensurability in gapless spin chains, that is described using a different fermion mapping [11].

For a long time the spin dynamics of Haldane-gap AFs in the high-field phase evaded direct experimental investigation by neutron scattering techniques. This was primarily due to large values of H_c for most known model quasi-1D integer-spin compounds. The situation changed with the discovery of $Ni(C_5D_{14}N_2)_2N_3(PF_6)$ (NDMAP), a material well suited for neutron scattering experiments and a critical field of only 5 T [12]. For $H > H_c$, residual interactions between the $S = 1$ Ni^{2+} chains in this compound lead to commensurate long-range AF ordering at low temperatures [12,13]. However, the strength of effective interchain coupling is about 0.2 meV, small compared to the in-chain exchange constant $J \approx 2.8$ meV [14,15]. At $\hbar\omega \gtrsim 0.2$ meV, one can thus directly study the exotic dynamics of the 1D model. In the present Letter, we report inelastic neutron scattering studies of low-energy excitations in NDMAP, for a magnetic field below and well above H_c, at temperatures above the 3D-ordered phase.

Experiments were carried out on the SPINS three-axis spectrometer installed at the cold neutron facility at the National Institute of Standards and Technology Center for Neutron Research. Twenty–three deuterated NDMAP single crystals were coaligned to produce a sample of total mass 1.2 g and a mosaic of about 7°. The sample was mounted in a cryomagnet and measurements were performed at $T = 2.5$ K and magnetic fields $H = 0$, 2, 4, 5.5, 7, and 9 T. The field was applied along the b axis of the orthorhombic structure (space group $Pnmn$), perpendicular to the spin chains that run along c (cell parameters $a = 18.05$ Å, $b = 8.71$ Å, $c = 6.14$ Å). The spectrometer employed a vertically focusing pyrolitic graphite (PG) (002) monochromator and a 23 cm × 15 cm flat multiblade PG(002) analyzer positioned 91.4 cm from the

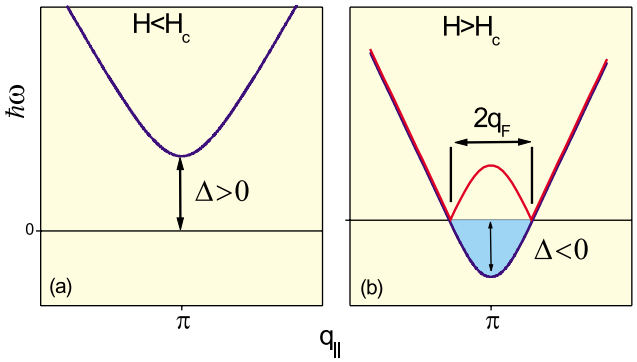

FIG. 1 (color). Dispersion in the lowest-energy Haldane-gap mode below (a) and above (b) the critical field H_c (blue). In the free-fermion model, excitations with a negative energy at $H > H_c$ form a Fermi sea (shaded area) with a characteristic Fermi vector q_F. Lowest-energy excited states are viewed as "particles" for $|q_\parallel - \pi| > q_F$ or "holes" for $|q_\parallel - \pi| < q_F$ (red line).

sample. Scattered neutrons were registered by a position-sensitive detector (PSD). Measurements were done with fixed-final neutron energy for the central analyzer blade of 3.1 meV. The collimation setup was (^{58}Ni-guide)-(open)-(open)-80'(radial), and a Be filter was used either before or after the sample. To minimize the contributions of the sample mosaic to wave vector resolution, all scans were performed such that momentum transfer for the center pixel of the PSD was along c^*. Wave vector transfer along c^* will be denoted by $q_\parallel$. In a single setting of the spectrometer, the PSD covered an energy range of 1 meV and a range of wave vector transfer along the chain of $0.3c^*$. Separate scans were corrected for the analyzer efficiency, and merged to produce a single data set. A linear background was subtracted from each constant-E slice taken from the data set at each field. The data were smoothed using a Gaussian kernel with $\delta E = 0.05$ meV FWHM and $\delta q_\parallel = 0.01c^*$. Typical resulting data sets are visualized in Fig. 2.

For the following discussion it is important to estimate the critical field H_c. Long-range ordering, that is essentially a three-dimensional (3D) effect and occurs at $H_c^{3D} \approx 12$ T for $T = 2.5$ K, is of little interest in the present study. The relevant quantity is the field $\tilde{H}_c$ at which the gap for the lower-energy Haldane excitation vanishes at $\boldsymbol{q} = (0, 0, 0.5)$, where all the measurements were performed. $\tilde{H}_c$ can be estimated from the gap energies measured in zero field [14] and the known gyromagnetic ratio for the ($S = 1$)-carrying Ni^{2+} ions in NDMAP [12]. Using Eq. (2.14) in Ref. [16] we get $\tilde{H}_c \approx 7.3$ T. Below, we shall first review the results obtained for $H < \tilde{H}_c$, and proceed to discuss the 9 T data that represent the high-field phase and contain our most important findings.

The Haldane triplet in NDMAP is split by single-ion anisotropy [14]. The parabolic shape seen in Fig. 2(a) for $H = 0$ corresponds to two lower-energy gap excitations polarized along the a and b axes, with gap energies $\Delta_1 = 0.48(1)$ meV and $\Delta_2 = 0.65(1)$ meV, respectively. The experimental resolution is not sufficient to resolve these two modes. The gap in the c-axis polarized Haldane excitation, $\Delta_3 \approx 1.9$ meV [14], is outside the energy range covered in the present experiment. In Fig. 2(b), at $H = 5.5$ T, one clearly sees the splitting of the doublet. Excitations polarized along the b axis (upper branch) are $S_z = 0$ states, z being chosen along the applied field. To first order, they are not affected by the magnetic field. The gap for the a-axis polarized Haldane excitation (lower mode) decreases with field by virtue of the Zeeman effect.

The data were analyzed using a parametrized model cross section, numerically convoluted with the calculated spectrometer resolution. Details of the data analysis will be given elsewhere and only the main points are summarized here. The cross section was written in the single mode approximation [14]. For each observed excitation branch, the dispersion relation was written as $(\hbar\omega_{\boldsymbol{q}})^2 = \Delta^2 + v^2 \sin^2(\boldsymbol{qc})$ (model 1). The gaps and intensities for each branch were adjusted to best fit the experimental data. At each field the *entire* data set with energy transfers between 0.2 and 1.6 meV was analyzed with a single set of parameters in a *global* fit. The spin wave velocity v was fixed at $v = 6.9$ meV, as determined at $H = 0$. The model was found to describe the data measured at up to 7 T very well, with a residual $\chi^2 < 1.5$ in all cases. The obtained field dependence of the gap energies is plotted in

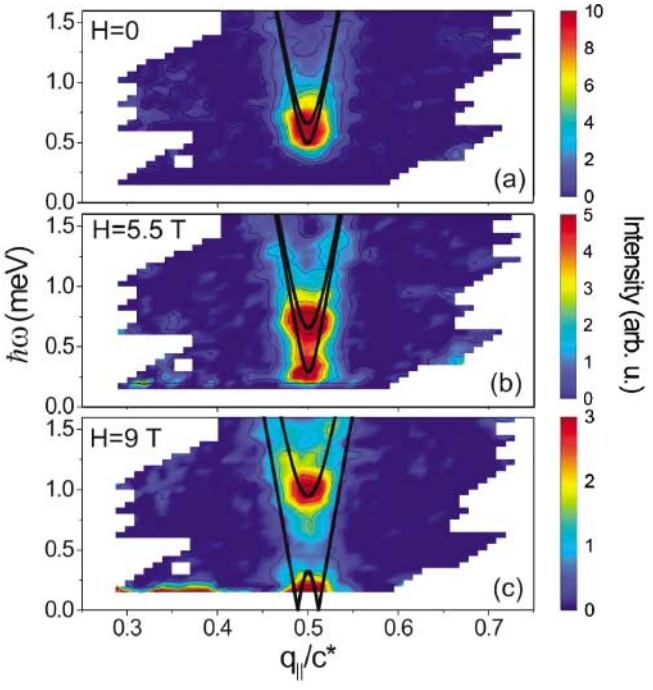

FIG. 2 (color). False color plots of inelastic intensity measured in NDMAP at $T = 2.5$ K for different values of magnetic field applied along the b axis. The extra intensity seen below $q_\parallel = 0.4c^*$ at low energies in (c) is most likely an artifact of imperfect background subtraction. Solid lines are as described in the text.

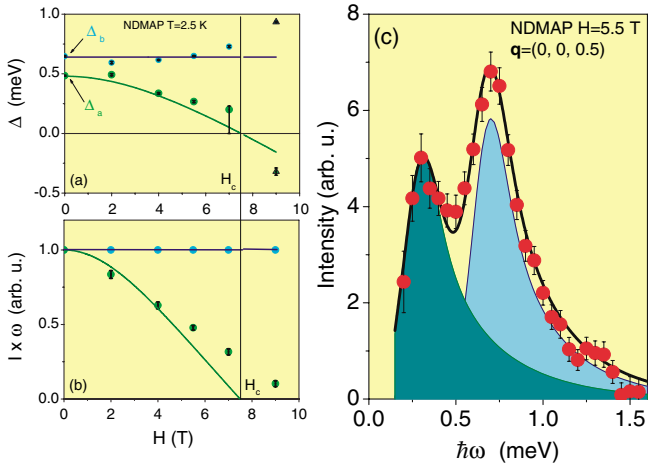

FIG. 3 (color). Field dependence of the gap energies (a) and excitation intensities (b) measured in NDMAP at $T = 2.5$ K (symbols). (c) A constant-Q scan collected at $H = 5.5$ T (symbols). Solid lines and shaded areas are as described in the text.

Fig. 3(a). The corresponding dispersion relations are shown as solid lines in Figs. 2(a) and 3(b). Figure 3(c) shows a constant-Q scan extracted from the 5.5 T data set (symbols) plotted over the profile simulated using the refined parameter values (solid line). The shaded areas show partial contributions from the two gap modes. Similarly, Figs. 4(a)–4(c) show a series of extracted constant-E scans for $H = 5.5$ T, plotted on top of the corresponding simulated profiles (solid lines). The measured field dependence of gaps follows the general trend [solid lines in Fig. 3(a)] expected from a perturbation treatment of the Zeeman term [16]. In agreement with the perturbation analysis [blue line in Fig. 3(b)], the measured intensity of the upper mode is field independent [Fig. 3(b), cyan symbols] while that of the lower mode decrease with H as it acquires polarization along the c direction to which our experiment is insensitive [Fig. 3(c), green line]. At $H < \tilde{H}_c$ the behavior is well described by first order perturbation theory and is similar to that previously found in the extensively studied Haldane-gap compound $Ni(C_2H_8N_2)_2NO_2(ClO_4)$ (NENP) [17].

We now turn to the data visualized in Fig. 2(c), collected at $H = 9$ T $> \tilde{H}_c$. The gap in the upper mode has increased substantially, to about 0.93 meV, as compared to 0.63 meV at $H = 5.5$ T. Interestingly, below this gap, a weak but well-defined area of scattering extends all the way down to the lowest accessible energy transfer. Because of limited wave vector resolution and the steep $1/\omega$ intensity scaling, the dispersion of these excitations is difficult to discern other than by a quantitative analysis (see below). This is not conventional critical scattering associated with the imminent phase transition, as the experiment was done away from $\mathbf{Q}_c = (h, 0.5, 0.5)$ where magnetic Bragg peaks appear below T_N. This first experimental observation of quasi-one-dimensional quasielastic neutron scattering for $H > H_c$ implies that individual spin chains in NDMAP are in a critical phase from which quasi-long-range order would likely emerge on cooling even in the absence of interchain coupling.

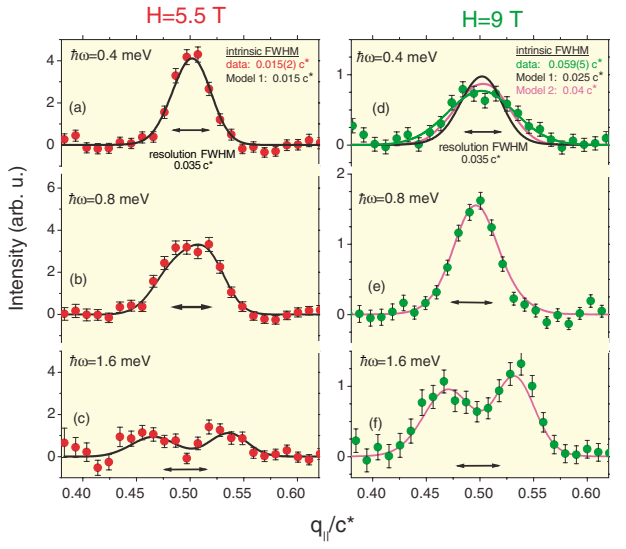

FIG. 4 (color). Symbols: Constant-E scans collected in NDMAP at $H = 5.5$ T $< \tilde{H}_c$ [(a)–(c)] and $H = 9$ T $> \tilde{H}_c$ [(d)–(f)]. Lines are as described in the text. Arrows indicate the projection of the resolution ellipse onto the chain axis.

Closer examination of the data reveals important changes at high fields beyond closing the gap in the neutron scattering spectrum. Applying the low field analysis procedure to the 9 T data yields a significantly worse fit ($\chi^2 = 2.0$) than was achieved for $H < \tilde{H}_c$. The problem is mainly in the wave vector and energy dependence of inelastic scattering at low energies. The discrepancy is particularly pronounced in the shape of constant-E scans, where the data shows peaks considerably broader than simulations based on parameters obtained in the fit. To quantify this behavior, we scaled the measured intensity by the energy transfer and integrated the result over the range 0.25–0.5 meV. The resulting q dependence was fit to a Gaussian profile to obtain an intrinsic (resolution corrected) width of $0.048(5)c^*$. The peak simulated using parameters determined in the global fit has an intrinsic width of only $0.023c^*$. The anomalous q width is also visible in each measured constant-E scan individually, as, for example, at 0.4 meV energy transfer [Fig. 4(d)]. It is important to emphasize that the discrepancy is *not* related to an error in resolution calculation. Indeed, at lower fields, e.g., at $H = 5.5$ T [Fig. 4(a)], Gaussian fits to constant-E scans and simulated profiles yield identical widths. Moreover, even at $H = 9$ T at higher energy transfers, where the dominant contribution is from the 0.93 meV mode, the model cross section fits the data quite well [Figs. 4(e) and 4(f), solid lines].

At least two theoretical frameworks could potentially account for the $q_\parallel$-broadened quasielastic scattering in the high field phase of NDMAP. A classical easy plane antiferromagnet with a field in the easy plane can be mapped onto a Sine-Gordon model with a gapped spin wave spectrum and topological soliton excitations [18]. While solitons have a finite rest mass, they are stable topological objects that move freely along the spin chain. The soliton gas yields quasielastic neutron scattering with a $q_\parallel$ width that varies in proportion to the soliton density. The soliton model was used successfully to account for the phase diagram of NDMAP with fields normal to the chain axis [19]. In addition, soliton pinning at defects may account for the quasi-two-dimensional frozen state in NDMAP for fields perpendicular to the easy plane [13]. Further evaluation of the Sine-Gordon model for the high field phase of NDMAP would require measurements of the H/T dependence of the $q_\parallel$ width for comparison to the theoretical soliton density. The free-fermion model presented in the introduction describes a different type of topological excitations. In this model at $H > H_c$ the lowest energy excitations with momentum transfers along the chains near $q_\parallel = \pi/c$ are single-particle or single-hole states. These have a dispersion relation as shown by the red line

in [Fig. 1(b)]. To compare the 9 T data to the free-fermion model, we constructed an empirical dispersion relation for the lower mode [model 2] with q_F as a new parameter. The dispersion was assumed to be linear outside the region $\pi/c - q_F < q_\parallel < \pi/c + q_F$, and to follow half a period of a sine wave within these boundaries. The prefactor for the sinusoidal part was chosen to give the correct spin wave velocity at $q_\parallel = \pi/c \pm q_F$. As illustrated in Fig. 1(b), a given value of q_F corresponds to a "negative gap" $\Delta = -2q_F c v/\pi$. With $q_F = 0.03(1)c^*$ [$\Delta = -0.3(1)$ meV], model 2 yields a considerably better agreement with experiment ($\chi^2 = 1.3$) than model 1. The refined gap energy for the upper mode and the negative gap for the lower branch are indicated with triangles in Fig. 3(a). Simulations based on resulting parameter values are shown in magenta lines [Figs. 4(d)–4(f)], and the dispersion relations are shown in a solid line in Fig. 2(c). While at high energies where the upper mode is dominant the two models are virtually indistinguishable, below 0.6 meV transfer model 2 does a better job at reproducing the observed peak widths [Fig. 4(d)].

The free-fermion model makes a very robust prediction for the field dependence of q_F. The Fermi vector q_F determines the number of $S_z = 1$-carrying particles present in the ground state at $H > H_c$ and is therefore directly proportional to the uniform magnetization: $M = g\mu_B 2q_F/c^*$, where M is the magnetization per spin. For NDMAP, the magnetization curve has been measured experimentally [20] and at 9 T $M \approx 0.1\mu_B/Ni^{2+}$. This gives $q_F = 0.025c^*$, remarkably close to the experimental value. It is important to stress that the free-fermion model is a rather crude approximation. In fact, at $H > H_c$ the system is to be described as a sea of *interacting* fermions, i.e., a *Luttinger liquid* (for a recent discussion see Ref. [7]). As a result of these interactions, there is no well-defined Fermi surface or even single-particle poles in the dynamic susceptibility. Incommensurate correlations are obscured: The equal-time spin correlation function is a broad peak at the commensurate $q_\parallel = \pi$ point. It is probably for this reason that *static* long-range ordering in NDMAP [13] and the related compound $Ni(C_5H_{14}N_2)_2N_3(ClO_4)$ (NDMAZ) [21] is commensurate. In the Luttinger liquid model, the low energy excitations are a continuum. Experimental evidence for this behavior was recently obtained in studies of NDMAP [19] and NENP [22]. While the resolution of our experiments on NDMAP is insufficient to distinguish between continuum and single-particle excitations, the free-fermion model appears to be a good starting point for the data analysis. It can reproduce the measured data quite well, and yields a *self-consistent* estimate for q_F.

In summary, our experiments demonstrate $q_\parallel$-broadened quasielastic scattering in the high-field phase of a $S = 1$ Haldane-gap compound. Various models based on topological excitations with low energy phase fluctuations may account for the data, including the Sine-Gordon and the free-fermion models. Further theoretical and experimental work will be required to identify the correct description of the high field phase in the anisotropic spin-1 chain.

We would like to thank I. Zaliznyak, A. Tsvelik, I. Affleck, and S. Sachdev for illuminating communications, and R. Rothe (BNL) for technical assistance. Work at BNL and ORNL was carried out under DOE Contracts No. DE-AC02-98CH10886 and No. DE-AC05-00OR22725, respectively. Work at JHU was supported by the NSF through DMR 9801742. Experiments at NIST were supported by the NSF through DMR-9413101. Work at RIKEN was supported in part by a Grant-in-Aid for Scientific Research from the Japanese Ministry of Education, Culture, Sports, Science and Technology.

*Present address: Solid State Division, Oak Ridge National Laboratory, Oak Ridge, Tennessee 37831-6393.

[1] F. D. M. Haldane, Phys. Lett. **93A**, 464 (1983).
[2] H. J. Schulz, Phys. Rev. B **34**, 6372 (1986).
[3] I. Affleck, Phys. Rev. B **41**, 6697 (1990); Phys. Rev. B **43**, 3215 (1991).
[4] M. Takahashi and T. Sakai, J. Phys. Soc. Jpn. **60**, 760 (1991); M. Yajima and M. Takahashi, J. Phys. Soc. Jpn. **63**, 3634 (1994).
[5] P. P. Mitra and B. I. Halperin, Phys. Rev. Lett. **72**, 912 (1994).
[6] T. S. S. Sachdev and R. Shankar, Phys. Rev. B **50**, 258 (1994).
[7] R. M. Konik and P. Fendley, cond-mat/0106037.
[8] K. Katsumata *et al.,* Phys. Rev. Lett. **63**, 86 (1989).
[9] A. M. Tsvelik, Phys. Rev. B **42**, 10 499 (1990).
[10] N. Fujiwara *et al.,* Phys. Rev. B **47**, 11 860 (1993).
[11] E. Pytte, Phys. Rev. **10**, 4637 (1974); G. Muller *et al.,* Phys. Rev. B **24**, 1429 (1981); D. C. Dender *et al.*, Phys. Rev. Lett. **79**, 1750 (1997).
[12] Z. Honda, H. Asakawa, and K. Katsumata, Phys. Rev. Lett. **81**, 2566 (1998).
[13] Y. Chen *et al.,* Phys. Rev. Lett. **86**, 1618 (2001).
[14] A. Zheludev *et al.,* Phys. Rev. B **63**, 104410 (2001).
[15] Y. Koike *et al.,* J. Phys. Soc. Jpn. **69**, 4034 (2000).
[16] O. Golinelli, T. Jolicoeur, and R. Lacaze, J. Phys. Condens. Matter **5**, 7847 (1993).
[17] L. P. Regnault *et al.,* Phys. Rev. B **50**, 9174 (1994).
[18] H. J. Mikeska and M. Steiner, Adv. Phys. **40**, 191 (1991).
[19] Z. Honda *et al.,* Phys. Rev. B **63**, 064420 (2001).
[20] Z. Honda *et al.,* Physica (Amsterdam) **284B–288B**, 1587 (2000).
[21] A. Zheludev, Z. Honda, K. Katsumata, R. Feyerherm, and K. Prokes, Europhys. Lett. **55**, 868 (2001).
[22] I. Zaliznyak *et al.* (to be published).